Photothermal Methods and Atomic Force Microscopy Images Applied to the Study of Poly(3-Hydroxybutyrate) and Poly(3-Hydroxybutyrate-*co*-3-Hydroxyvalerate) Dense Membranes

L. H. Poley,[1] A. P. L. Siqueira,[1] M. G. da Silva,[1] R. Sanchez,[2] R. Prioli,[3] A. M. Mansanares,[4] H. Vargas[1]

[1]*Laboratório de Ciências Físicas–LCFIS, Universidade Estadual do Norte Fluminense, Centro de Ciências e Tecnologia, Av. Alberto Lamego, 2000, 28015-620 Campos dos Goytaczes-RJ, Brazil*
[2]*Laboratório de Materiais Avançados–LAMAV, Universidade Estadual do Norte Fluminense, Centro de Ciências e Tecnologia, Av. Alberto Lamego, 2000, 28015-620 Campos dos Goytacazes–RJ, Brazil*
[3]*Departamento de Física–Pontifícia Universidade Católica do Rio de Janeiro, Rua Marques de São Vicente, 225 Gávea, Rio de Janeiro, RJ, Brazil*
[4]*Instituto de Fisica Gleb Wataghin Universidade Estadual de Campinas, CX, P.6165, CEP 13083-970-Campinas, SP, Brazil*

Received 2 September 2004; accepted 10 December 2004
DOI 10.1002/app.21891
Published online in Wiley InterScience (www.interscience.wiley.com).

ABSTRACT: Thermal and transport properties of some polyhydroxyalkanoates (PHAs), poly-3- hydroxybutyrate and poly-3-hydroxybutyrate-*co*-3-hydroxyvalerate copolymers at different concentrations (8, 14, and 22%), were studied by using photoacoustic and photothermal techniques. Mass diffusion coefficients were obtained for carbon dioxide and oxygen by using a gas analyzer. Specific heat capacity measurements were performed by monitoring temperature of the samples under white light illumination against time. Thermal diffusivities were determined by using the open photoacoustic cell configuration. The results were discussed considering the incorporation of hydroxyvalerate units in the poly(3-hydroxybutyrate) unit cell and were correlated with atomic force microscopy images of the upper surface of membranes. New information on transport properties of PHAs is provided. © 2005 Wiley Periodicals, Inc. J Appl Polym Sci 97: 1491–1497, 2005

Key words: diffusion coefficient; thermal diffusion; photoacoustic spectroscopy

INTRODUCTION

Photoacoustic (PA) spectroscopy and related photothermal techniques are well-established techniques. They are based on the generation of heat as a result of absorption of a modulating radiation.[1,2] For characterization of materials, photothermal techniques are a powerful tool. Some applications that should be mentioned are determination of thermal properties of ceramics[3] and polymers,[4] study of vapor diffusion in air,[5] and recently, determination of diffusion coefficients in polymers.[6] Advantages of PA and photothermal techniques include their simplicity, requirement of minimal sample preparation, high sensitivity, and applicability to a wide range of materials, including biological specimens.[7]

Measurement of the transport of gases and vapors in polymers is an important subject from both a technological and a scientific point of view. Applications include protective coatings, packing materials for food and beverages, and selective barriers for gas or liquid mixtures.[8] Some examples of experimental methods presented in the literature for measuring permeability and diffusion coefficients in polymers are gravimetric methods,[9] FTIR,[10] UV fluorescence,[11] and electrochemical techniques.[12]

Poly-3-hydroxybutyrate (PHB) and poly-3-hydroxybutyrate-*co*-3-hydroxyvalerate (PHB-*co*-HV) are members of a family of thermoplastic polyesters obtainable from renewable resources such as glucose and propionic acid through bacterial activity.[13] They seem to be very suitable for application in the food (plastic packages) and drug industry (controlled release of pharmaceuticals),[14] areas for which the studies of transport of gases and vapors are crucial. This theme was contemplated in some works in the literature such as the study of water, carbon dioxide, and vapor permeation using gravimetric techniques,[15,16] effect of membrane preparation on its transport properties,[17] and synthesis of membranes for ultrafiltration.[18]

Correspondence to: H. Vargas (vargas@uenf.br).
Contract grant sponsor: CAPES.
Contract grant sponsor: FAPERJ.
Contract grant sponsor: CNPq.

The present work intends to offer new knowledge about short-chain polyhydroxyalkanoate dense membranes, studying its diffusion coefficients to oxygen and carbon dioxide and their thermal properties using photoacoustic techniques. The results are correlated with topographic AFM images and surface analysis data.

EXPERIMENTAL

Sample preparation

Polymers used in this study were PHB and three copolymers, with nominal content of 3-hydroxyvalerate (3HV) of 8, 14, and 22%, all purchased from Aldrich Chemical Co., Inc. (Milwaukee, WI) They were first purified by dissolution in chloroform and precipitation in methanol. Dense films of polymers were prepared by casting chloroform solution (1% m/m) in a 15 × 22 cm glass plate. Evaporation took place in a closed glass chamber at 20°C. The chamber had a small outlet (1 cm) to control the vapor solvent flow into air. These procedures impose a careful control of evaporation to obtain a homogeneous dense film. After complete evaporation of solvent, each film was stored at atmospheric conditions for 24 h to the complete crystallization process. Film thickness was obtained from an average of 20 measurements. Films with a thickness of 60 μm were chosen to perform the measurements.

X-ray diffraction

Membranes crystallinity studies were performed by wide-angle X-ray diffraction. A Seifert-FPM model URD65 X-ray generator with a Ni filter to provide CuK_α radiation was used. Every scan was recorded in the range of 2θ from 5° to 40° with an exposure time of 10 s. Crystalline and amorphous regions of the diffractogram were fitted to Gaussians and crystallinity degree was calculated from the ratio of areas corresponding to these regions.

Thermal analysis

Membranes were thermally analyzed in a differential scanning calorimeter (DSC 2010, TA Instruments). Indium was used as calibration reference. Samples of 10 mg were encapsulated in aluminum pans and heated from −90 to 190°C at 20°C min^{-1}. Glass transition, melting temperature, and enthalpy of fusion were determined.

Mass diffusion coefficient measurements

The experimental setup applied for mass diffusion coefficient measurements consists of two chambers sealed off one from another by the analyzed membrane. The permeate gas in the study (oxygen and carbon dioxide) was introduced on one side and kept at a constant pressure of 4.9 Pa by means of a needle valve. The concentration of the diffused gas into the second chamber was measured by using a photoacoustic gas analyzer (URAS 14 from ABB) for carbon dioxide and an analyzer based on the paramagnetic properties of oxygen (Magnos 16 from ABB), both interfaced to a computer for data acquisition. Assuming Fick's model for mass diffusion, the time evolution for the permeate concentration in the analysis chamber is given by[5]

$$C = C_0(1 - e^{-t/\tau_D}) \quad (1)$$

where C_0 is the gas concentration at saturation regime, $\tau_D = l_s^2/2D$ is the gas diffusion time, D is the gas diffusion coefficient, and l_s is the sample thickness. Thus, by monitoring the time evolution of the gas concentration, the gas diffusion time, τ_D, was determined and, then, the diffusion coefficient D. All experiments were carried out at 25°C.

Heat capacity measurement

The heat capacity per unit of volume, ρc_p, was measured by using the temperature rise method under continuous white-light illumination. Samples were painted on both surfaces with a very thin film of black paint and were adiabatically suspended in a Dewar flask, which was subsequently vacuum-sealed ($\approx 10^{-2}$ Pa). Under these conditions, the main heat-loss mechanism takes place by radiation. The Dewar flask has an entrance glass window through which the continuous white-light beam was focused onto one of the sample surfaces. A thermocouple was attached on the opposite surface by using thermal paste. In this way, the temperature evolution of the back surface could be monitored as a function of time. The rear surface temperature rise is given by[19]

$$\Delta T = (I_0\tau/l_s\rho c_p)(1 - e^{-t/\tau}) \quad (2)$$

where I_0 is the intensity of the incident light and $\tau = l_s\rho c_p/(2H)$ is the rise temperature time, $H = 4\sigma T_0^3$ is the radiative heat-transfer coefficient, where σ is the Stefan–Boltzmann constant and T_0 is the ambient temperature. The parameter τ, from which the specific heat capacity is determined, fits the exponential data with eq. (2).

Thermal diffusivity

The thermal diffusivity, α_s, was measured by using the PA technique. This technique looks directly at the heat generated in a sample, due to thermal relaxation pro-

TABLE I
Crystallinity and Thermal Parameters Obtained for PHAs

Sample	Glass transition temperature (°C)	Melting temperature (°C)	Enthalpy of fusion (J/g)	Crystallinity (%)
PHB	2.4	176	101.5	64
P(HB-8%HV)	−1.1	159	142.4	62
P(HB-14%HV)	−4.0	151	42.6	61
P(HB-22%HV)	−4.8	158	24.9	59

cess, following the absorption of light. Among several techniques, the open photoacoustic cell (OPC) method was used. It consists of mounting the samples directly onto a cylindrical electret microphone and using the front air chamber of the microphone itself as the usual gas chamber of conventional photoacoustics. Further details of the experimental arrangement used can be found in the literature.[1,3]

For solid samples, three different mechanisms, which are responsible for the photoacoustic signal, typically exist; thermal diffusion, thermal expansion, and thermolelastic bending.[1] In the case of our samples, the thermolelastic mechanism is dominant. Thermal diffusivity was obtained from the fitting of experimental phase data to the following expression, valid when the thermoelastic sample bending is the dominant contribution to the PA signal:

$$\phi = \phi_o + \arctan\left(\frac{1}{x-1}\right) \tag{3}$$

where $x = l_s\alpha_s = l_s(\pi f/\alpha_s)^{1/2}$, l_s is the sample thickness, and α_s is its thermal diffusivity. In the derivation of eq. (3), it is assumed that the sample is optically opaque and that the heat flux into the surrounding air is negligible. The implicit optical opaqueness condition was ensured by the use of a thin circular absorbing Al foil (14-μm-thick and 5-mm-diameter) attached to the front surface of the sample using a thin layer of vacuum grease. The thermal diffusion time in this Al foil is about 13.6 μs so that the heat generated in the thin Al absorber can be assumed to be instantaneously transmitted to the sample.

To complete sample thermal characterization, knowing α_s and ρc_p, sample thermal conductivity, k, is readily obtained from the equation

$$k = \alpha_s \rho c_p \tag{4}$$

AFM images

To characterize membrane morphology previously to gas diffusion experiments, topographic atomic force microscopy (AFM) images of the upper surface of membranes were obtained by using a multimode scanning probe microscope with a nanoscope IIIa controller supplied from Digital Instruments (USA). Tapping mode of operation was used to eliminate shear forces that may damage the membranes and reduce the image resolution. Images were undertaken in air at 25°C.

RESULTS AND DISCUSSION

Crystallinity and thermal analysis

Table I presents the values obtained for membrane crystallinity and values of glass transition, melting temperature, and enthalpy of fusion obtained from the DSC measurements. As the hydroxyvalerate content increases, crystallinity tends to decrease slightly, as a consequence of the greater difficulty to accommodate polymer chains in the crystalline phase due to the presence of the ethyl group in the monomer hydroxyvalerate. Thermal parameters also decrease, reflecting a lower crystallization rate and the existence of irregular and complex crystals.

Mass diffusion coefficients

In Figure 1(a,b), the gas concentration in the analyzer chamber is presented as a function of time for CO_2 and O_2, respectively. Gas concentration increases asymptotically, reaching a saturation threshold. The solid lines in these figures represent the best fit of experimental data using eq. (1). This fitting allowed the determination of the characteristic mass diffusion time, τ_D, and then the diffusion coefficients of the membranes. A typical CO_2 mass diffusion coefficient value of 1×10^{-9} cm^2/s was found for PHB. Figure 2(a) shows the four different samples characterized in this work and their respective values of diffusion coefficient.

Figure 2(a) also compares carbon dioxide diffusion coefficients obtained in this work with those obtained in a previous work[16] (cross symbols) using conventional gravimetric techniques for membranes prepared under similar conditions. Both results indicate the same tendency, therefore, validating the methodology employed here. Applying a similar procedure of

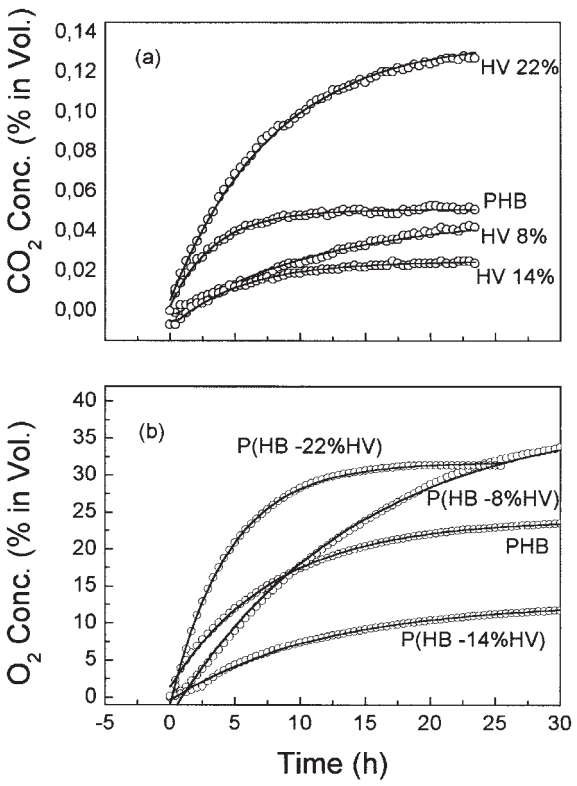

Figure 1 Concentration evolution for (a) CO_2 and (b) O_2. The solid line represents the best fit of the experimental data to eq.(1) using τ_D as an adjustable parameter.

analysis, in Figure 2(b), oxygen diffusion coefficients are plotted as a function of hydroxyvalerate concentration. It can be noted that these coefficients increase for polymers with higher hydroxyvalerate contents, reflecting the slight decrease in crystallinity as discussed above for these polymers.

Thermal properties

In Figure 3(a), the increasing time evolution of temperature for the copolymer P(HB-14%HV) sample after establishment of sample illumination and time evolution during cooling, when the illumination is switched off, are shown. The solid lines represent the best fit of experimental data using eq. (2) by using τ as an adjustable parameter, from which the values of specific thermal capacity can be obtained.

In Figure 3(b), values of specific heat capacity are plotted as a function of hydroxyvalerate concentration. There is a nearly linear decreased tendency of heat capacity with the hydroxyvalerate concentration. It is already known that the incorporation of hydroxyvalerate in the crystalline unit cell of PHB occurs without changes in the crystalline phase density and with a linear decrease in amorphous phase density.[20] Thus, the heat capacity behavior with the hydroxyvalerate concentration reflects the reduction of the amorphous phase density. However, in view of the magnitude of specific heat capacity diminishing (almost 35%), it is likely that other factors may be contributing. An additional interpretation would take into account the presence of air in the free volume of the polymers. Considering the results of oxygen and carbon dioxide mass diffusion [Figs. 2(a, b)], it is reasonable to assume that air solubility of samples grows with increasing hydroxyvalerate concentration. As air-specific heat capacity is 1.17×10^{-3} J cm^{-3} K^{-1}, three orders of magnitude lower than the values in the typical range of polymers, therefore, air could, under these conditions, contribute to a stronger reduction in heat capacity values.

Measurements of the dependence of the photoacoustic signal on the modulation frequency (not shown) show for all studied samples a signal amplitude variation close to f^{-1}. This feature supports the finding that the thermoelastic sample bending is the dominant mechanism for the acoustic signal generation.[4] In Figure 4(a), PA signal phase data as a function of modulation frequency for the P(HB- 8% HV) sample are shown. The solid curve in this figure corresponds to the experimental data fitting [eq. (3)], with an error of 5%. The same procedure was applied to the others samples.

Figure 4(b) shows that the thermal diffusivity values increase with increasing hydroxyvalerate concentration, reaching a saturation threshold at $\approx 1.7 \times 10^{-3}$

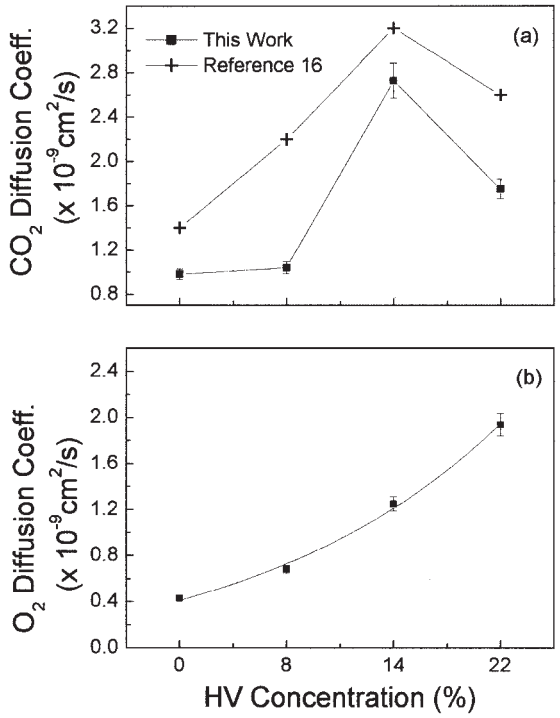

Figure 2 Mass diffusion coefficient as a function of the hydroxyvalerate concentration: (a) for CO_2 (filled squares) and compared with those reported previously[16] (cross symbols) and (b) for oxygen.

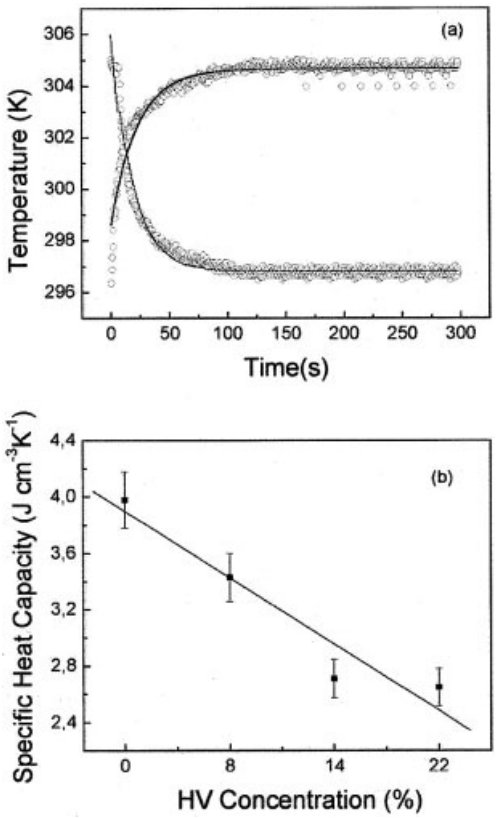

Figure 3 (a) Time evolution of the temperature on the back surface of the sample. The solid lines represent the best fit of the experimental data applying eq. (2), used as an adjustable parameter. (b) The dependence of the specific heat capacity on the concentration of hydroxyvalerate.

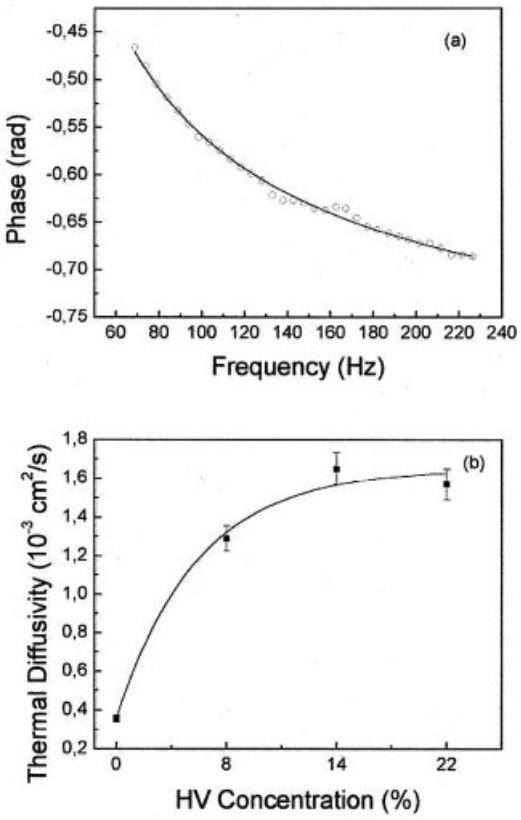

Figure 4 (a) Dependence of the phase of the photoacoustic signal on the modulation frequency. Each solid line represents the best fit of eq. (3), using τ as the thermal diffusion coefficient as adjustable parameter. (b) The thermal diffusivity as a function of the concentration of hydroxyvalerate.

cm^2/s. These values are slightly higher than those reported by previous authors,[21] who also observed the tendency for saturation of thermal diffusivity. The differences can be attributed to the sample preparation procedure. For PHB, the order of magnitude of its thermal diffusivity (10^{-4} cm^2/s) agrees with its already reported piezoelectric properties.[22] Likewise, in the discussion developed for heat capacity, these results can be discussed considering that the presence of air in the free volume inside the polymers should be responsible for the increase of thermal diffusivity. This effect is justified by the thermal diffusivity of air (0.22 cm^2/s), which is at least two orders of magnitude higher than those obtained for polymers. Adding to this, the increase of distances among polymer chains in the amorphous phase decreases thermal diffusivity, as observed by some authors,[23] and thus may compensate the influence of air, generating the saturation effect observed in Figure 4(b). The fitting of experimental data to an exponential growing function led to an empirical relation between thermal diffusivity and hydroxyvalerate concentration in the range of 0–22% as follows:

$$\alpha = 0.00166 - 0.0013e^{-HV/5.652} \quad (5)$$

Thermal conductivity of samples, calculated from the values of thermal diffusivity and specific heat capacity [eq. (4)], is presented in Figure 5. The behavior is similar to that observed for thermal diffusivity and can be interpreted in the same way. Table II summarizes experimental results for thermal and transport characterization of samples.

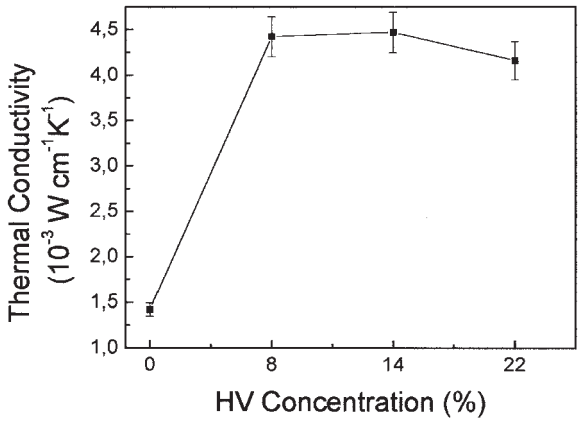

Figure 5 The thermal conductivity dependence on the concentration of hydroxyvalerate.

TABLE II
Mass Diffusion Coefficients and Thermal Properties of Membranes

Sample	Thermal diffusivity ($\times 10^{-3}$ cm^2/s)	Specific heat capacity (J/cm^3 K)	Thermal conductivity ($\times 10^{-3}$ W/cm^2 K)	D_{O_2} ($\times 10^{-9}$ cm^2/s)	D_{CO_2} ($\times 10^{-9}$ cm^2/s)
PHB	0.36 ± 0.02	3.98 ± 0.20	1.42 ± 0.14	0.43 ± 0.02	0.98 ± 0,05
P(HB-8%HV)	1.29 ± 0.06	3.43 ± 0.17	4.42 ± 0.4	0.68 ± 0.03	1.04 ± 0.05
P(HB-14%HV)	1.65 ± 0.07	2.71 ± 0.14	4.47 ± 0.5	1.25 ± 0.06	2.73 ± 0.14
P(HB-22%HV)	1.57 ± 0.07	2.65 ± 0.13	4.16 ± 0.4	1.94 ± 0.1	1.75 ± 0.09

AFM images

Figure 6 shows AFM topographic images of the upper surface of membranes studied. A rough surface with topographic highs and reliefs can be identified, which is similar to the morphology described in literature for membranes prepared by spin coating using scanning electron microscopy (SEM).[18,24] From Figure 6, it can also be observed that as hydroxyvalerate concentration increases, so does the size of depressions, and their number decrease. To analyze these differences in a quantitative way, the following roughness parameters of the images were calculated using the AFM software program:

1. The difference between the highest and the lowest points within the given area, z;
2. The standard deviation of the z values within the given area, R_q;
3. The mean roughness, R_a.

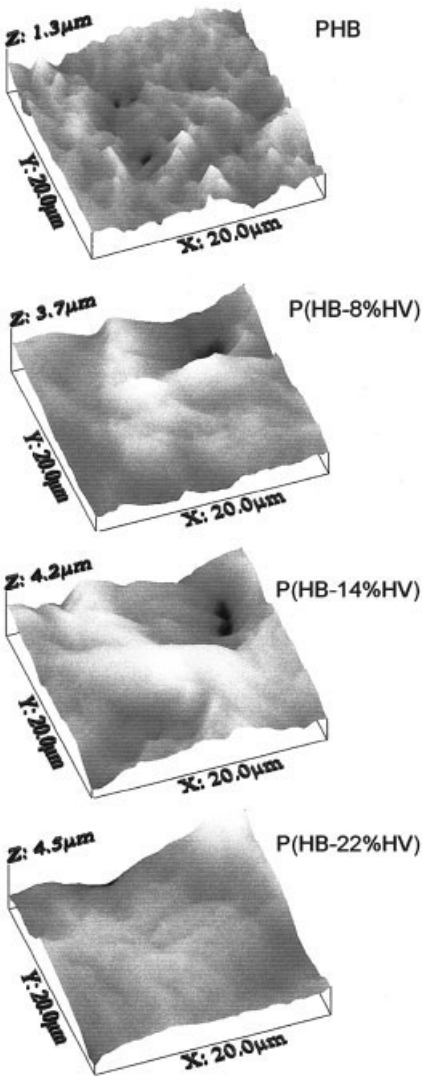

Figure 6 AFM topographic images of the upper surface of the membranes.

Table III summarizes the roughness parameters of the membranes. All parameters increase with hydroxyvalerate concentration. If compared to the results of diffusion coefficient, it can be observed that the increase of roughness parameters corresponds to an increase of diffusion coefficients. This fact agrees with the observations of some authors[25] in the study of water permeability and surface morphology of cellulose acetate membranes and evidences the intrinsic relation between membrane transport properties and their morphology.

CONCLUSION

In this article, we have reported on the measurements of the thermal and sorption properties of polyhydroxyalkanoates films prepared by casting using the PA techniques. The results demonstrate the sensitiveness of thermal properties to the internal structure of the material and allowed the establishment of empirical relations between thermal properties and 3-hydroxyvalerate content. Morphology observed in AFM

TABLE III
Roughness Parameters of Membranes

Sample	R_a (μm)	R_q (μm)	z (μm)
PHB	0.18	0.15	1.30
P(HB-8%HV)	0.64	0.43	3.65
P(HB-14%HV)	0.81	0.80	4.24
P(HB-22%HV)	0.60	0.55	4.48

images and values of roughness parameters demonstrated good agreement with gas diffusion results.

The authors thank Brazilian agencies CAPES, FAPERJ, and CNPq for financial support of this work.

References

1. Vargas, H.; Miranda, L. C. M. Phys Rep 1998, 161, 43.
2. Almond, D.; Patel, P. Photoacoustic and Photothermal Science and Techniques; Chapman and Hall: London, 1996.
3. Alexandre, J.; Marín, E.; Marques, B.C; Ribeiro, M.; Salles, C.; Silva, M.G.; Sthel, M. S.; Auler, L.; Vargas, H. Analyst 1999, 124 (8), 1209.
4. Leite, N. F.; Cella, N.; Vargas, H.; L. C. M. Miranda, L. C. M. J Appl Phys 1987, 61, 3025.
5. Lima, J. A. P.; Silva, M. G.; Massunaga, M. S. O.; Marin, E.; Miranda, L. C. M. J Appl Phys 2002, 91, 5581.
6. Silva, M. G.; Gonçalves, S. S.; Sthel, M. S.; Schramm, D. U.; Sánchez, R.; Rieumont, J. B. Vargas, H. Rev Sci Instrum 2003, 74, 831.
7. Pereira, A. C.; Neto, G. O.; Vargas, H; Cella, N.; Miranda, L. C. M. Rev Sci Instrum 1994, 65, 1512.
8. Marais, S.; Saiter, J. M.; Devallencourt, C.; Nguyen, Q. T.; Métayer, M. Polym Test 2002, 21, 425.
9. C. J. Guo, C. J.; De Kee, D.; Harrison, B. J Appl Polym Sci 1995, 56, 823.
10. Musto, P.; Mascia, L.; Ragosta, G.; Scarinzi, G.; Villano, P. Polymer 2000, 41, 564.
11. Pekcan O.; Ugur, S. Polymer 2000, 41, 7531.
12. Compañ, V.; Ribes, A.; Díaz-Calleja, R.; Riande, E. Polymer 1998, 37, 2243.
13. Doi, Y. Microbial Polyesters; VCH; New York.
14. Holmes, P. A. Phys Technol 1985, 14, 32.
15. Miguel, O.; Berridi-Fernandez, M. J.; Iruin, J. J. J Appl Polym Sci 1997, 64, 1849.
16. Miguel, O.; Barbari, T. A.; Iruin, J. J. J Appl Polym Sci 1999, 71, 2391.
17. Iordanskii, A. L.; Kamaev, P. P.; Hanggi, U. J. J Appl Polym Sci 2000, 76, 475.
18. Mas, A.; Jaaba, H.; Sledz, J.; Schue, F. Eur Polym J 1996, 32, 435.
19. Hatta, I. Rev. Sci Instrum 1979, 50, 292.
20. Mitomo, H.; Morishita, N.; Doi, Y. Polymer 1995, 36, 2573.
21. Sánchez, R. R.; Rieumont, J. B.; Cardoso, S. L.; Silva, M. G.; Sthel, M. S.; Massunaga, M. S. O.; Gatts, C. N.; Vargas, H. J Brazilian Chem Soc 1999, 10, 97.
22. Zhang, D. M.; Cui, F. Z.; Luo, Z. S.; Lin, Y. B.; Zhao, K.; Chen, G. Q. Surf Coat Technol 2000, 131, 350.
23. Agari, Y.; Ueda, A.; Omura, Y.; Nagai, S. Polymer 1997, 38, 801.
24. Galego, N.; Miguens, F. C.; Sánchez, R. Polymer 2002, 43, 3109–3114.
25. Stamatialis, D. F.; Dias, C. R.; Pinho, M. N. J Membrane Sci 1999, 160, 235.